

Manipulating the quantum information of the radial modes of trapped ions: Linear phononics, entanglement generation, quantum state transmission and non-locality tests

Alessio Serafini,^{1,2} Alex Retzker,^{2,3} and Martin B. Plenio^{2,3}

¹ Department of Physics & Astronomy, University College London, Gower Street, London WC1E 6BT, UK

² Institute for Mathematical Sciences, 53 Prince's Gate, Imperial College London, London SW7 2PG, UK

³ QOLS, Blackett Laboratory, Imperial College London, London SW7 2BW, UK

Abstract. We present a detailed study on the possibility of manipulating quantum information encoded in the “radial” modes of arrays of trapped ions (*i.e.*, in the ions’ oscillations orthogonal to the trap’s main axis). In such systems, because of the tightness of transverse confinement, the radial modes pertaining to different ions can be addressed individually. In the first part of the paper we show that, if local control of the radial trapping frequencies is available, *any* linear optical and squeezing operation on the locally defined modes – on single as well as on many modes – can be reproduced by manipulating the frequencies. Then, we proceed to describe schemes apt to generate unprecedented degrees of bipartite and multipartite continuous variable entanglement under realistic noisy working conditions, and even restricting only to a global control of the trapping frequencies. Furthermore, we consider the transmission of the quantum information encoded in the radial modes along the array of ions, and show it to be possible to a remarkable degree of accuracy, for both finite-dimensional and continuous variable quantum states. Finally, as an application, we show that the states which can be generated in this setting allow for the violation of multipartite non-locality tests, by feasible displaced parity measurements. Such a demonstration would be a first test of quantum non-locality for “massive” degrees of freedom (*i.e.*, for degrees of freedom describing the motion of massive particles).

1. Prologue: the promise of alternative continuous variable degrees of freedom

The last decade saw a boom in the development of experimental capabilities available for quantum information processing. The ability to manipulate the information of discrete variables encoded in polarisation, spin and internal atomic degrees of freedom has by now reached very high standards. On the other hand, the control and manipulation of continuous variable (CV) quantum information is still almost exclusive to light fields in quantum optical settings. Even though purely optical systems rely on well established tools and are the natural choice for communication tasks over long distances, they also suffer from significant drawbacks. Notably, the entanglement generation in such systems is strongly limited by the efficiency of parametric processes in nonlinear crystals; moreover, ‘static’ optical degrees of freedom – *i.e.* light resonating in cavities – are seriously affected by losses and decoherence over their typical dynamical time scales.

Such limitations motivate the question of whether the full potential of infinite dimensional Hilbert spaces could be better harnessed by “massive” (*i.e.*, related to the position of a massive particle) CV degrees of freedom. Of course, to compete with the so far very successful quantum optical toolbox, such degrees of freedom would have to allow for a range of coherent manipulations at least as exhaustive as what quantum optics currently permits. Besides, to be considered advantageous over quantum optical systems, such degrees of freedom should allow for notable improvements in the generation of quantum entanglement and squeezed states under realistic working conditions.

In the present paper, we argue that trapped ions meet both such requirements, and present an extensive study to substantiate this argument. In particular, we shall focus on the radial motion of trapped ions, that is on oscillations along a direction orthogonal with respect to the array of ions. These oscillations are described by continuous variable quantum degrees of freedom which we will refer to as *radial modes* [1, 2]. Radial modes have attracted considerable interest in the last few years, mostly in view of the fact that they allow for a tighter confinement (which also permits one to define the phonons locally).

The paper is organised as follows. After having introduced the description of the physical system (Sec. 2), in Sec. 3 we demonstrate that any linear optical and squeezing operation can be obtained for radial modes of trapped ions by controlling the individual *radial* trapping frequencies, indicating that trapped ions can at least match the processing capabilities possible for light modes. In Sec. 4 we show that, even restricting to cases where only global control of the trapping potentials is possible, such systems are actually apt to outperform optical modes in the generation of entanglement, both bipartite and multipartite. As applications we consider, in Sec. 5, the propagation of quantum information along the array of ions, at both qubit and continuous variable levels and, in Sec. 6, the violation of multipartite non locality tests, and show them to be within the reach of current technology. Radial modes will thereby turn out to be promising not only for information processing but also as probes of fundamental physics.

2. The trap

We shall consider the radial modes of n ions of mass m and charge ze in a linear Paul trap [3]. Let \hat{X}_j and \hat{P}_j be the position and momentum operators associated to the radial degree of freedom of the j -th ion, which is trapped in the radial direction with angular frequency ω_j (see Fig 1). In the following, the *longitudinal* trapping frequency ω_L will be the unit of frequency and will set the unit of length as well (equal to $d = \sqrt[3]{z^2 e^2 / (4\pi \epsilon_0 m \omega_L^2)}$, where ϵ_0 is the dielectric constant); also, we shall set $\hbar = 1$, so that all the quantities will be dimensionless.

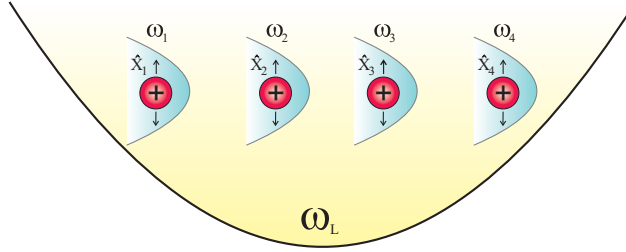


Figure 1. Considered setup: the ions are trapped along the longitudinal direction with the same trapping frequency ω_L . Also, each ion j is trapped along the transverse, ‘radial’ direction (*i.e.*, along the arrows in the drawing) with trapping frequency ω_j . The operator \hat{X}_j stands for the position of ion j along the radial direction: these radial oscillations are described by the modes $\{\hat{X}_j, \hat{P}_j\}$ we shall focus on.

The Coulomb interaction affects the local radial oscillation frequencies: for convenience, let us then define the ‘effective’ local radial frequencies

$$\tilde{\omega}_j = \omega_L \sqrt{\frac{\omega_j^2}{\omega_L^2} - \sum_{l \neq j} \frac{d^3}{|u_j - u_l|^3}},$$

$\{u_j\}$ being the equilibrium positions of the ions [3]. Rescaling the canonical operators according to $\hat{x}_j = \sqrt{m\tilde{\omega}_j} \hat{X}_j$, $\hat{p}_j = \hat{P}_j / \sqrt{m\tilde{\omega}_j}$, and grouping them in a vector of operators $\hat{R} = (\hat{x}_1, \dots, \hat{x}_n, \hat{p}_1, \dots, \hat{p}_n)^T$, allows one to express the global Hamiltonian of the system in the harmonic approximation[†] as

$$\hat{H} = \frac{1}{2} \hat{R}^T (\boldsymbol{\kappa} \oplus \tilde{\boldsymbol{\omega}}) \hat{R}, \quad (1)$$

where $\tilde{\boldsymbol{\omega}}$ is a diagonal matrix: $\tilde{\boldsymbol{\omega}} = \text{diag}(\tilde{\omega}_1, \dots, \tilde{\omega}_n)$, while the potential matrix $\boldsymbol{\kappa}$ has diagonal entries $\kappa_{jj} = \tilde{\omega}_j$ and off-diagonal entries $\kappa_{jk} = \omega_L^2 d^3 / (\sqrt{\tilde{\omega}_j \tilde{\omega}_k} |u_j - u_k|^3)$ for $j \neq k$.

Let us recall the canonical commutation relations $[\hat{R}_j, \hat{R}_k] = i\Omega_{jk} \mathbb{1}$, where the $2n \times 2n$ matrix Ω has entries $\Omega_{j,k} = \delta_{n,k-j} - \delta_{n,j-k}$ for $1 \leq j, k \leq 2n$, and that Gaussian states are defined as states with Gaussian characteristic functions: a Gaussian state ϱ is thus uniquely determined by its ‘covariance matrix’ (CM) $\boldsymbol{\sigma}$, with entries given by

$$\sigma_{jk} \equiv \frac{1}{2} \text{Tr} [\{\hat{R}_j, \hat{R}_k\} \varrho] - \text{Tr} [\hat{R}_j \varrho] \text{Tr} [\hat{R}_k \varrho], \quad (2)$$

and by the vector of first moments R , with components $R_j \equiv \text{Tr} [\hat{R}_j \varrho]$ [4, 5].

The ground state of Hamiltonian \hat{H} is a Gaussian state with a block diagonal CM $\boldsymbol{\sigma}_g = (\boldsymbol{\sigma}_x \oplus \boldsymbol{\sigma}_x^{-1})/2$, where

$$\boldsymbol{\sigma}_x = \tilde{\boldsymbol{\omega}}^{1/2} (\tilde{\boldsymbol{\omega}}^{1/2} \boldsymbol{\kappa} \tilde{\boldsymbol{\omega}}^{1/2})^{-1/2} \tilde{\boldsymbol{\omega}}^{1/2},$$

and vanishing first moments.

[†] Notice that, in the harmonic approximation (*i.e.*, at second order in the ions’ displacements) the coupling between radial modes and longitudinal ones vanishes. Fourth order couplings are around 10^{-4} times smaller in the considered experimental conditions and will thus be safely neglected.

Finally, let us remember that the evolution for the time t of an initial Gaussian state with CM σ under a quadratic Hamiltonian $\hat{H} = \hat{R}^\top H \hat{R}$ (where H is any symmetric matrix) is a Gaussian state with CM given by

$$\sigma_t = S_t \sigma S_t^\top, \quad (3)$$

for $S_t = \exp(\Omega H t)$.

2.1. Dissipation

In our study, we will take into account the decoherence of the radial modes in an environment of phonons with temperature T and ‘loss rate’ γ (for simplicity assumed to be the same for every mode). Under such conditions, the evolution of the ions’ state ϱ at frequencies $\{\tilde{\omega}_j\}$ is described by the following master equation in interaction picture [6]

$$\frac{d\varrho}{dt} = \frac{\gamma}{2} \sum_{j=1}^n \left[N_j (2a_j^\dagger \varrho a_j - a_j a_j^\dagger \varrho - \varrho a_j a_j^\dagger) + (N_j + 1) (2a_j \varrho a_j^\dagger - a_j^\dagger a_j \varrho - \varrho a_j^\dagger a_j) \right], \quad (4)$$

where the number of phonons in the radial mode j is given by $N_j := 1 / \left(\exp\left(\frac{\hbar\tilde{\omega}_j}{k_B T}\right) + 1 \right)$, according to Bose law (k_B being Boltzmann constant) and $a_j := (\hat{X}_j + i\hat{P}_j)/\sqrt{2}$. In accordance with the experimental terminology, we will also refer to the quantity $\epsilon_j := N_j \gamma$ as the ‘heating rate’, essentially representing the rate at which thermal phonons are injected into mode j .

Eq. 4 preserves the Gaussian character of the initial state and can results, for the CM σ of Gaussian states, into the following equation:

$$\frac{d}{dt} \sigma = \gamma \sigma_\infty - \gamma \sigma$$

(where $\sigma_\infty \equiv \sigma' \oplus \sigma'$, $\sigma' = \text{diag}(N_1 + \frac{1}{2}, \dots, N_n + \frac{1}{2})$), with solution:

$$e^{-\gamma t} \sigma_t + (1 - e^{-\gamma t}) \sigma_\infty.$$

3. Linear phononics and beyond

In this section, we shall assume that the trapping frequencies $\{\omega_j\}$, and thus $\{\tilde{\omega}_j\}$, can be controlled locally and changed suddenly (*i.e.*, much faster than ω_j^{-1}). Such a local control may be achieved by building small, local radial electrodes, by adding local optical standing waves,[‡] or in trap arrays [7, 8]. Let us also note that a setting formally identical to the one we describe here could be reproduced shortly even for locally defined *axial* (‘longitudinal’) modes in segmented Paul traps [9]. The changes in trapping frequency we will consider (typically ranging between 1 and 10 MHz) can be realised in about 10ns [10], and will be regarded as instantaneous over our timescales. Our aim is to show how, in principle, local control of the frequencies allows one to perform any arbitrary ‘linear optical’ operation on the radial modes of the ions, that is any unitary operation under which, in the Heisenberg picture, the vector of operators \hat{R} transforms linearly: $\hat{R} \mapsto S \hat{R}$. The matrix S has to be ‘symplectic’, *i.e.* such that

$$S^\top \Omega S = \Omega$$

[‡] Currently, standing waves realize, at most, trapping potentials of about 1 MHz in experiments where the internal degrees of freedom are controlled. However, the manipulation of radial modes can tolerate much higher scattering rates than that of internal degrees of freedom, and would thus allow for much higher trapping frequencies.

(where Ω is the anti-symmetric symplectic form, defined at page 3), to preserve the canonical commutation relations. Notice that such a class of operators includes squeezing transformations.§ We should mention that the idea of squeezing the state of a single ion by controlling the trapping frequency was first put forward in the early 90's [11]. Also, single-mode squeezing can be achieved by coupling the motion of the ion with its internal degrees of freedom [12, 13]. The scope of the present Section is however wider, since we set out to prove that any symplectic operation on any number of ions can be implemented by frequency manipulation.

Let us first remark that any symplectic operation S on a system of many canonical degrees of freedom (“modes”) can be decomposed into a combination of generic single-mode symplectic transformations and two-mode rotations (“beam splitters”, in the quantum optical terminology) [14, 15]. This fact follows from the Euler decomposition of symplectic operations [14] and from the possibility of decomposing energy preserving operations into a network of beam-splitters between pairs of modes [15]. It is therefore sufficient for us to establish the possibility of performing these two subclasses of operations (single-mode symplectic transformations and two-mode beam splitters) on our system of n ions by manipulating the local frequencies. In turn, again because of Euler decomposition, single-mode operations can always be reduced to combinations of squeezings and phase-shifts.

3.1. Single mode operations

In what follows we assume that the original effective frequencies of the ions are different but commensurate, as given by, say, $\tilde{\omega}_j = j\tilde{\omega}$, and that $\tilde{\omega}$ is large enough so that interaction between any two ions is suppressed when the relevant coherent manipulation sets off.|| Let us then consider the reaction of the system if the frequency of the j -th ion changes suddenly from $\tilde{\omega}_j$ to $\alpha_j\tilde{\omega}_j$, for some real α_j (clearly, such changes are completely governed by changes in the ω_j 's). The Heisenberg equation of motion for \hat{x}_j and \hat{p}_j can be immediately integrated in such a case, resulting into a symplectic transformation $S_j(t)$ given by

$$S_j(t) = \begin{pmatrix} \alpha_j^{\frac{1}{2}} & 0 \\ 0 & \alpha_j^{-\frac{1}{2}} \end{pmatrix} \begin{pmatrix} \cos(\tilde{\omega}_j\alpha_j t) & \sin(\tilde{\omega}_j\alpha_j t) \\ -\sin(\tilde{\omega}_j\alpha_j t) & \cos(\tilde{\omega}_j\alpha_j t) \end{pmatrix} \begin{pmatrix} \alpha_j^{-\frac{1}{2}} & 0 \\ 0 & \alpha_j^{\frac{1}{2}} \end{pmatrix}. \quad (5)$$

The first and last matrix of this decomposition correspond to ‘squeezing’ operations in the quantum optical terminology, whereas the second factor is known as a ‘phase shift’ (*i.e.*, a rotation in the single-mode phase space). Combinations of squeezings and phase-shifts make up any possible single-mode symplectic operation: we thus need to show that such operations can be implemented individually on any ion of the system in a controllable manner (as pointed out above, this is sufficient because of the Euler decomposition of single mode operations [14]).

§ In the literature, squeezing transformations have a tendency to be excluded from the class of “linear” transformations, because their implementations require ‘nonlinear’ (third order) interactions. However, the effective evolution of the modes of interest (‘signal’ and ‘idle’, usually) is actually linear in the sense specified above (linear evolution of the vector \hat{R} in Heisenberg picture), and we will thus generally refer to ‘linear’ transformations as including squeezing.

|| The linear scaling of the coupling is not a stringent requirement. Because the coupling between ion j and k falls off like $|j - k|^{-3}$, one can safely assume, say, a ‘triangle’ profile (alternately increasing and decreasing) for the couplings in long chains of ions. Note also that, for a linear scaling, the population of the levels of ion j due to the interaction with k roughly scales as $1/(1 + (\tilde{\omega}/\omega_L)^2|j - k|^5)$: a frequency step $\tilde{\omega} \simeq 20\omega_L$ is already enough to make the effects of all the interactions essentially negligible.

3.1.1. Phase-shift To realise a phase-shift operation on the k -th ion, without any squeezing, it is sufficient to change the frequencies of all the other ions in the same way, such that, in the notation defined above, $\alpha_k = 1$ and $\alpha_j = \alpha \neq 1$ for $j \neq k$ (α_j being the factor by which the frequency of ion j is multiplied by manipulating the local trapping potential). As apparent from Eq. (5), after a time $t_\alpha = 2\pi/(\tilde{\omega}\alpha)$ from the change one has $S_j = \mathbb{1}_2$ for $j \neq k$: all the ions which undergo a change in trapping frequency are back to their initial state (let us recall that $\tilde{\omega}_j = j\tilde{\omega}$ by assumption, so that after t_α the central rotation of Eq. (5) reduces to the identity and the two opposite squeezing transformations just nullify each other). On the other hand, the transformation S_k will be equal to the central rotation (with no squeezing, as α_k is kept equal to 1) of angle $\varphi_k = 2\pi k/\alpha$: the oscillation of the k -th ion will have acquired such a phase, analogous to the “optical phase” of light modes. If the frequencies are switched back to the original values after a time t_α , the net effect of the evolution is then analogous to an ‘optical’ phase-shift of angle φ_k on the ion k .

3.1.2. Squeezing In order to squeeze the state of ion k , leaving all the other ions unaffected, one can conversely change only the pertinent frequency, so that $\alpha_k \neq 1$ and $\alpha_j = 1$ for $j \neq k$. Then, after a time period $t = 2\pi/\tilde{\omega}$, all the other ions will have returned to the initial state, while ion k will be squeezed and phase-shifted according to Eq. (5). The phase-shift can always be arbitrarily corrected by applying the strategy to obtain “pure” phase shifts described in Sec. 3.1.1, which conclusively shows that *any linear operation on a single mode can be implemented by controlling the local trapping frequencies.*¶

The degree of squeezing achievable with such a strategy depends crucially on the phase-shift operation since, as shown by Eq. (5), the two squeezing operations act along orthogonal directions and are the inverse of each other. In the case $\alpha_k = (\frac{1}{4} + h)/k$ for $h \in \mathbb{N}$, the two squeezings act effectively along the same phase space direction: in this instance the phase-shift can be balanced by a counter-rotation of $\pi/4$ in phase space and the final squeezing operation is a diagonal matrix given by $\text{diag}(\alpha_k, \alpha_k^{-1})$. In principle, the value of α_k is only limited by the stability of the system and the breakdown of the harmonic approximation [2], occurring when the squeezing is comparable to the ratio between the size of the wave packet and the distance between the atoms. In actual experiments, the considered setup would thus allow for $\sqrt{\alpha_k} \ll 500$. Notice that such values are by far out of reach in optical systems, where squeezings corresponding to $\alpha_k \simeq 8$ were recently reported [16]. Also notice that, by placing the ions inside cavities, the squeezing of the massive degrees of freedom could be transferred to light, so that radial modes could act as an effective source of squeezing (and potentially even entanglement) for optical systems as well [17].

3.1.3. Beam-splitters To extend our proof to any linear operation, on any number of ions, let us now turn to ‘beam-splitting’ operations between the radial modes of any two ions in the array. Such operations are achieved by bringing the two modes in question (hereafter labeled by j and k) to the same frequency $\tilde{\omega} = \tilde{\omega}_j = \tilde{\omega}_k$, so that the Coulomb interaction between them is no longer suppressed. Switching to the interaction picture, one has the following coupling Hamiltonian between the two modes:

$$\hat{H}_I = \kappa_{jk} \hat{x}_j(t) \hat{x}_k(t) = \kappa_{jk} (a_j e^{-i\tilde{\omega}t} + a_j^\dagger e^{i\tilde{\omega}t}) (a_k e^{-i\tilde{\omega}t} + a_k^\dagger e^{i\tilde{\omega}t}),$$

¶ In fact, arbitrary adjustment of the phase allows for “pure” squeezing operations along the phase space directions x and p , and thus implies the possibility to construct any linear operation, because of the symplectic Euler decomposition previously discussed.

where the ladder operators are defined as $\hat{x}_j = (a_j + a_j^\dagger)$ and κ_{jk} is an entry of the matrix κ defined in Eq. (1). If the frequency $\tilde{\omega}$ is sufficiently large the rotating wave approximation reliably applies and the rotating terms can be neglected to yield⁺

$$\hat{H}_I = \kappa_{jk}(a_j a_k^\dagger + a_j^\dagger a_k) .$$

This Hamiltonian realises exactly the desired beam splitter-like evolution, resulting into a symplectic transformation which mixes \hat{x}_j with \hat{x}_k and \hat{p}_j with \hat{p}_k (rotating such pairs equally, by the angle $\kappa_{jk}t$). For instance, a ‘50 : 50’ beam splitter is achieved after a time $t = \pi/(4\kappa_{jk})$. Since the interaction requires a change of the local frequencies it includes automatically in it a local operation, which may however be corrected before or after the ‘beam-splitting’ procedure, as detailed above.

Summing up, the combined arguments presented in Secs. 3.1.1, 3.1.2 and 3.1.3 show that *any “linear optical” operation*, including squeezing operations and entangling operations acting on multiple different modes, *can be implemented for radial modes of trapped ions by properly tuning the frequencies of the radial microtraps of the individual ions.*

Linear optical operations, complemented by displacements (see Sec. 3.2), correspond to all the unitary transformations that preserve the Gaussian character of the initial state. Therefore, all the developments based on Gaussian states in quantum optics, in particular concerning entanglement manipulation [4] and information protocols [18], can be carried over to radial modes of ion traps if local control is achieved. Arguably, the framework we have outlined for the implementation of linear optical operations on the local oscillations of distinct ions, to which one may refer as “linear phononics”, could offer further practical advantages over its quantum optical counterparts, essentially related to the static nature of the quantum information processed (for instance, ‘mode matching’, which hampers substantially the implementation of linear optics, is not a problem here).

3.2. Further manipulations and measurements

Beside the linear operations treated so far, implemented through varying trapping potentials and Coulomb interactions, the motional degrees of freedom of trapped ions allow for other controlled manipulations, some of which take advantage of the coupling between motion and the internal degrees of freedom that can be engineered by applying standing- or traveling-wave pulses to the ions. In order to give a complete account of the possibilities offered by radial modes, let us here review such strategies, and briefly comment about their applicability to radial modes. As a general remark let us mention that, because of the tighter confinement they allow for, radial modes easily meet the Lamb-Dicke condition (depending on the width of the ground state’s wavepacket), which means that the coupling with the internal degrees of freedom can be tailored to a high degree of accuracy (generally better than for longitudinal modes).^{*} Also, individual ions can be addressed in such manipulations as, at spacings of some micrometers and assuming pulses’ waists of the order of $1 \mu\text{m}$, less than 1% of the central laser power would be shined on neighbouring ions with respect to the central one.

Displacement operations, which shift the operators \hat{R}_j by real numbers, can be realized in several ways: by classical driving fields, by standing waves, or by shifting the radial equilibrium positions of the ions [19]. In particular, transverse driving fields could be applied to displace the radial modes, with no particular hurdles. In the following, the unitary

⁺ This always holds at the trapping frequencies we shall consider in specific examples, going from 1 to few tens of MHz, for which stability around 10^{-3} are achievable.

^{*} The price to pay for such an accuracy is longer operation times, which could be ultimately reduced if stronger lasers became viable.

displacing the canonical operators of mode j by, respectively, x_j and p_j will be denoted by $\hat{D}_j(x_j, p_j)$.

Notably, even *non-Gaussian* states can be engineered in this setup with relative ease (with respect to quantum optics, where non-Gaussian manipulations require higher order nonlinearities, usually extremely weak), either by entering the nonlinear regime of the Coulomb interactions or by coupling the internal degrees of freedom of the ions. The experimental realisation of a cross-Kerr coupling for the longitudinal oscillations of trapped ions has been recently reported [2].

The coupling to internal degrees of freedom also allows for Gaussian and non Gaussian measurements on individual ions. The measurement of quadrature operators, corresponding to *homodyning*, was proposed in [20, 21, 22]. Quantum non-demolition measurement of local number states and parity could be measured as well, by applying the scheme suggested and realised for cavity QED in [23], based on the dispersive coupling of the number of oscillations to two internal levels of the ion. Quite remarkably, such a scheme would allow one to measure the phonon number's parity on a single copy of the state and run of the apparatus. As we will see in Sec. 6, this possibility is consequential for the violation of Bell-like inequalities. Notice also that such non-Gaussian measurements pose a considerable technological challenge for light fields, where resolving photon numbers with high detector efficiency is still daunting despite recent progress [24, 25]. On the other hand, the schemes recalled above are bound to be comparatively slow, requiring to wait for half a period of coherent interaction between motions and internal levels and then subsequent readout of the internal levels by, *e.g.*, fluorescence. When internal degrees of freedom are involved, radial modes require longer times, roughly on the order of tens of microseconds, but achieve remarkable precision.

Finally, concerning the preparation of initial states for coherent manipulations, let us remind that cooling of ion oscillations to their ground state can be achieved very efficiently by sideband-Raman pulses [26, 27] (or more recent variations over such a strategy [28, 29]). Note, since in the described scenario the initial local potential is much larger than the interaction, simultaneous cooling of all the chain could be done by cooling each ion to its local ground state, which is to a good approximation the global ground state. The local single excitations on such ground states may be prepared by addressing the first ion with a proper sequence of blue and red sideband pulses, as detailed in [19].

In the remainder of the paper we shall demonstrate the potential of linear operations on radial modes in specific applications, with a particular focus on settings fully accessible to current experiments.

4. Entanglement generation

The set of operations described in Sec. 3, including local squeezing and two-mode beam splitters between distant modes, allows for the generation of entanglement between the radial modes of two ions in the chain. In fact, as is well known, two single-mode states squeezed along orthogonal quadratures, entering a beam splitter, give rise to an entangled state for the outgoing modes (this is a standard procedure to create CV entanglement in quantum optics). In principle, for the system of trapped ions under examination, the local control of the transverse trapping frequencies allows for the creation of tailored entangled states, where the entanglement can be build up between any two ions in the chain. Moreover, and possibly even more intriguingly, the possibility of controlling a system of n parties (the ions) all constantly interacting with each other, paves the way for the creation of *multipartite*

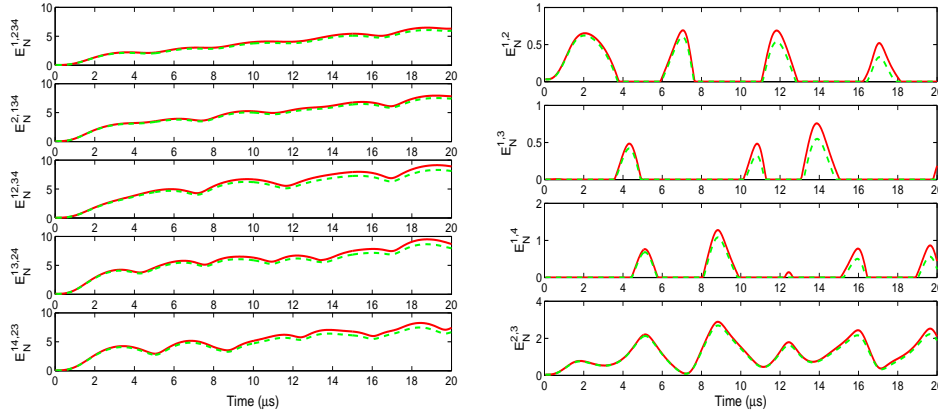


Figure 2. Dynamics of the entanglement (in ebits of logarithmic negativity) between the radial modes of the ions, in a trap containing $n = 4$ ions and with longitudinal trapping frequency $\omega_L = 1\text{MHz}$. At time $t = 0$ the system starts off from the ground state for transverse trapping frequency $\omega_i = 5\text{MHz}$ and then evolves under a trapping frequency $\omega_f = 2\text{MHz}$. The plots on the left show the logarithmic negativity shared by all the possible bipartitions of the four modes (because of the spatial symmetry, one has only five distinct cases in the chain: for instance, one has $E_N^{1,234} = E_N^{4,123}$). On the right, the logarithmic negativity shared by pairs of modes is plotted (again, because of symmetry, there occur only four distinct cases). The continuous (red) curves refer to a case with no dissipation, while the dashed (green) curves refer to a case with heating rate $\epsilon = 2\text{KHz}$ (resulting from a coupling to the bath $\gamma = 10^{-4}\text{Hz}$ and a temperature $T = 294^\circ\text{K}$).

entanglement between the distinct ions.

In this section we show that unprecedented degrees of bipartite entanglement, as well as interesting and robust multipartite entangled states, can be obtained in settings accessible to current experiments, starting from a ground state of the system and *requiring only global control of the trapping potential* (where, *i.e.*, the trapping frequencies $\{\omega_j\}$ are the same for all ions at any time, and are only changed simultaneously). Further, we will briefly discuss the possibilities a local control of the frequencies that would open up for the controlled dynamics of multipartite entanglement.

The specific situation we shall address starts off from the ground state ρ_g of Hamiltonian \hat{H} [see Eq. (1)] – with all frequencies being equal, *i.e.* $\omega_j = \omega_i$ for $1 \leq j \leq n$ – as the initial state. Next, the trapping frequencies are changed to the common value ω_f , so that the state ρ_g will not be stationary anymore under the modified Hamiltonian. For large ω_i , the initial state ρ_g contains very little entanglement but, if the frequencies are suddenly changed, entanglement builds up during the subsequent evolution (see [30] for an analogous scheme in chains of nanomechanical oscillators). Entanglement between different subsystems will be quantified by the logarithmic negativity $E_N \equiv \log_2 \|\tilde{\rho}\|_1$, where $\|\tilde{\rho}\|_1$ stands for the trace norm of the ‘partially transposed’ density matrix of the subsystem [31, 5]. Different partitions will be denoted by superscripts referring to the ions: for instance, the logarithmic negativity between ions 1-2 and 3-4 will be denoted by $E_N^{12,34}$. The intuition behind this entanglement generation method is that operating faster than the speed of sound in the system, *i.e.*, essentially, faster than the inverse of the energy gaps, is analogous to operating locally. Thus, by changing the local potentials (in the same way for each ion) fast enough one generates local squeezing, which is then ‘converted’ into entanglement by the time-evolution

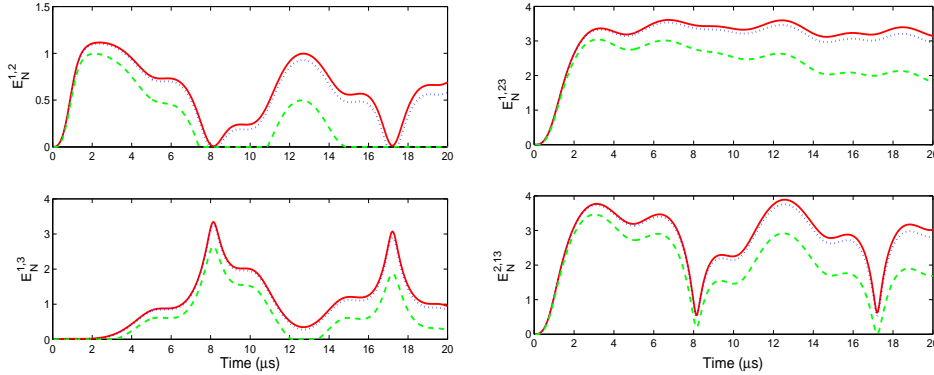


Figure 3. Dynamics of the entanglement (in ebits of logarithmic negativity) between the radial modes of the ions, in a trap containing $n = 3$ ions and with longitudinal trapping frequency $\omega_L = 1\text{MHz}$. At time $t = 0$ the system starts off from the ground state for transverse trapping frequency $\omega_i = 20\text{MHz}$ and then evolves under a trapping frequency $\omega_f = 2\text{MHz}$. The plots on the left show the logarithmic negativity shared by all the possible bipartitions of the four modes (because of the spatial symmetry, one has only two distinct cases in the chain). On the right, the logarithmic negativity shared by pairs of modes is plotted (again, because of symmetry, there occur only two distinct cases). The continuous (red) curves refer to a case with no dissipation, the dotted (blue) curves refer to a case with heating rate $\epsilon = 200\text{Hz}$ (resulting from a coupling to the bath $\gamma = 10^{-5}\text{Hz}$ and a temperature $T = 294^\circ\text{K}$), while the dashed (green) curves refer to a case with heating rate $\epsilon = 2\text{KHz}$ (resulting from a coupling to the bath $\gamma = 10^{-4}\text{Hz}$ and a temperature $T = 294^\circ\text{K}$).

through the harmonic coupling between the ions, analogous to a set of beam splitters.

The case portrayed in Fig. 2 represents four ions starting from the ground state for $\omega_i = 5\text{MHz}$, which then evolves under the frequency $\omega_f = 2\text{MHz}$ for $20\mu\text{s}$ (for a transverse trapping frequency $\omega_L = 1\text{MHz}$). As can be seen, the global state gets entangled under any possible bipartition of the four modes, a situation which is referred to in the literature as “complete inseparability” [32]. A more extensive inspection shows that this is a general property of the Hamiltonian at hand, even for larger number of ions. Of course, as shown in Fig. 3, complete inseparability also occurs for three ions: in Sec. 6 we shall see how the multipartite entanglement for three ions analysed in Fig. 3 could serve to violate Bell-like inequalities. Our plots also show that such an entanglement exhibits considerable resilience under realistic heating rates. In this respect, notice that the heating rate for the dashed (green) curved plotted in the graphs is $\epsilon = 2\text{KHz}$, and that heating rates as low as $\simeq 10\text{Hz}$ have been recently observed in ion traps (even though for a single ion only [33, 34]): robust multipartite entanglement (between 5 and 10 ebits of logarithmic negativity) between the ions can thus be created. Such degrees of entanglement are inconceivable for multipartite systems in photonic systems where, furthermore, the manipulation of several modes tends to become awkward due to the increasing number of mode-matching conditions to be fulfilled.

In the plots, we also report the entanglement of pairs of modes in the traps for four, three and two ions. For bipartite entanglement as well, as shown in Fig. 4, the degree of robust entanglement achievable is by far beyond the maximal values obtained in quantum optical systems,[‡] even considering rather modest frequency jumps. The case portrayed in

[‡] To the best of our knowledge, the highest *measured* value for the logarithmic negativity in optical systems (inferred from state reconstruction) is $E_{\mathcal{N}} \simeq 1.6$ ebits [35]. A simple evaluation also shows that, exploiting the degree of squeezing reported in [16] and assuming *perfect* beam-splitting operations, one could achieve at most $E_{\mathcal{N}} \lesssim 3$ ebits.

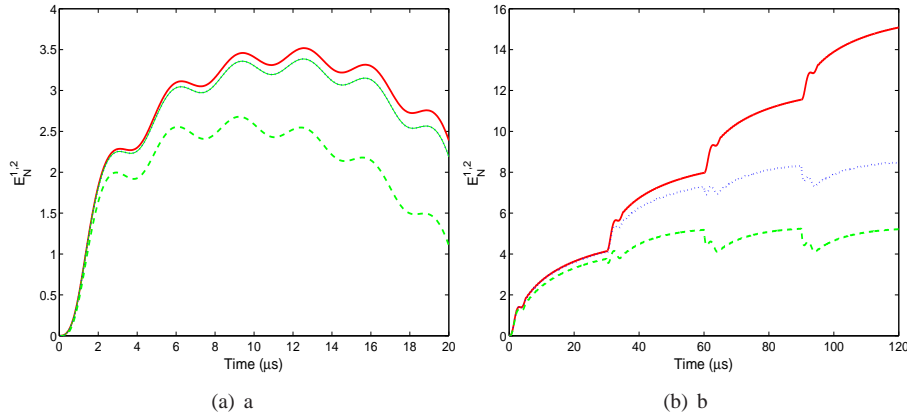


Figure 4. Dynamics of the entanglement (in ebits of logarithmic negativity) between the radial modes of the ions, in a trap containing $n = 2$ ions and with longitudinal trapping frequency $\omega_L = 1\text{MHz}$. In plot (a), the system starts off from the ground state for transverse trapping frequency $\omega_i = 20\text{MHz}$ and then evolves under a constant trapping frequency $\omega_f = 2\text{MHz}$. In plot (b), the initial frequency is $\omega_i = 20\text{MHz}$ and then the system evolves for $5\ \mu\text{s}$ at frequency $\omega_f = 2\text{MHz}$ and for $25\ \mu\text{s}$ at frequency ω_i ; for iterations of the cycle are displayed. The continuous (red) curves refer to a case with no dissipation, the dotted (blue) curves refer account for a heating rate $\epsilon = 200\text{Hz}$, while the dashed (green) curves refer to a case with heating rate $\epsilon = 2\text{KHz}$ (resulting from a coupling to the bath $\gamma = 10^{-4}\text{Hz}$ and a temperature $T = 294^\circ\text{K}$).

Fig. 4(b) starts from the ground state for $\tilde{\nu}_i = 10\text{MHz}$. Afterwards, the frequency is switched to $\omega_f = 2\text{MHz}$ for $5\ \mu\text{s}$ and then back to ω_i for $25\ \mu\text{s}$: such a cycle realizes a highly entangling operation because it is tailored such that the squeezings act always in the same phase-space directions and, in principle, can be iterated at will to obtain any desired degree of entanglement. In practice decoherence and dissipation will degrade such an entanglement after some iterations. However, as is apparent from the plot, stable and robust entanglement (around 10 ebits of logarithmic negativity) between two ions could be created under realistic conditions.

Also, in the traps with more than two ions, the dynamics of the entanglement between pairs of modes displays a ‘monogamous’ behaviour [36]: for four ions, when the entanglement between ions 1 and 2 fades, the entanglement between 1 and 3 starts raising and then is replaced by entanglement between 1 and 4, which in turn fades out before the revival of the quantum correlations between 1 and 2. The entanglement between 2 and 3 – strongly favoured by the fact that such ions are both nearest neighbours *and* at perfect resonance with each other (not true in general, as the Coulomb corrections on the trapping frequencies depend on the position in the trap) – is always positive but, significantly, its peaks and dips follows those of the entanglement between 1 and 4, as one would heuristically expect by virtue of monogamy. As reminded above, the reported values of ω_i and ω_f represent the ‘bare’ trapping frequencies, not taking into account the corrections due to Coulomb repulsion: therefore, the ions are not all at resonance during the evolution. Now, if one assumes that local control were available, one could correct for such a mismatch by applying different bare frequencies to ions in different positions along the trap’s longitudinal axis. We applied such corrections in the four ions case considered above and found that, quite interestingly, one can spread correlations more evenly in this way and get closer to the ultimate bounds imposed by monogamy: after

$10\mu\text{s}$ (all the parameters being the same aside from the corrections) one ends up with a state where each radial mode is individually entangled with all the other radial modes (a situation which never arises without corrections, see Fig. 2).

The continuous variable entanglement between two radial modes of the ions could be swapped to light if cavities were added to the setup, with the potential to achieve unprecedented degrees of optical entanglement, as the parametric processes are definitely outperformed by the strategy outlined above based on the trapping frequency's control: this possibility will be the subject of a detailed investigation in a forthcoming paper [17].

5. Propagation of quantum information

The locally defined radial modes of the ions, interacting via the Hamiltonian (1), are an example of *harmonic chain*, where the coupling between different oscillators can be, to a very good extent, controlled. The propagation of quantum information in such a setting has been proposed and analysed theoretically in [37], but not yet realised in practice since mechanical oscillators have yet to enter the quantum regime (due to the technical difficulties still encountered in controlling both the couplings and the decoherence and dissipation of chains of nano-oscillators [38]). Trapped ions could thus provide a very promising alternative to implement harmonic chains, realize quantum data buses [39] and test the results predicted by theoretical studies. More generally, such a demonstration would be a further application of ion traps as *quantum simulators*, as already proposed in several past studies [40, 41]. In this Section, we shall present an overview of the possibilities offered by the radial modes as harmonic chains for the propagation of quantum states, with quantitative investigations, in scenarios similar to those detailed in the preceding sections.

5.1. Transmission of two-dimensional quantum states

The transmission of quantum information encoded in finite dimensional quantum states (most often qubit states) through a chain of interacting quantum systems has drawn much attention in recent years [42], as such systems are envisaged as possible quantum buses, linking different parts of future quantum processors. However, despite considerable efforts, finding systems where such a transmission can be realised with sufficiently small level of noise has proven to be very challenging. Therefore, good practical candidates for such tasks are still of interest. Proposals in this context have so far focused on the transmission of finite dimensional states in chains of interacting (effective or proper) 'spins'. Here, instead, we consider qubit states encoded in the bosonic Hilbert space of the radial modes of trapped ions and, guided by the results of the Section 3, we show that such modes are able to send qubit states through chains of trapped ions.

As a preliminary remark, let us notice that, if the ratio between the radial and the longitudinal trapping frequencies is very large, $\omega_j/\omega_L \gg 1 \forall j$, then the effect of the Coulomb interaction on the Hamiltonian governing the radial modes is negligible^{††} and the Hamiltonian (1) reduces to $\hat{H} \simeq \frac{1}{2}\hat{R}^\top\tilde{\omega} \oplus \tilde{\omega}\hat{R}$. That is to say, the radial oscillations of the individual ions are decoupled, with local normal frequencies approximately given by $\{\omega_j\}$. In this situation, the ground state of the system is just the ordinary, non-squeezed, vacuum: a Gaussian state with CM equal to the identity and vanishing first moments. For instance, for $\omega_j = 50\omega_L \forall j$ the relative discrepancy between the actual ground state and the vacuum is only 10^{-3} in terms of covariances. Starting from such a ground state, we will consider a scenario where

^{††}See page 3 and notice that, quite remarkably, the ratios $d/|u_j - u_k|$ does not depend on the trapping frequencies nor on the masses of the ions but only on the total number of ions n (see [3] for details).

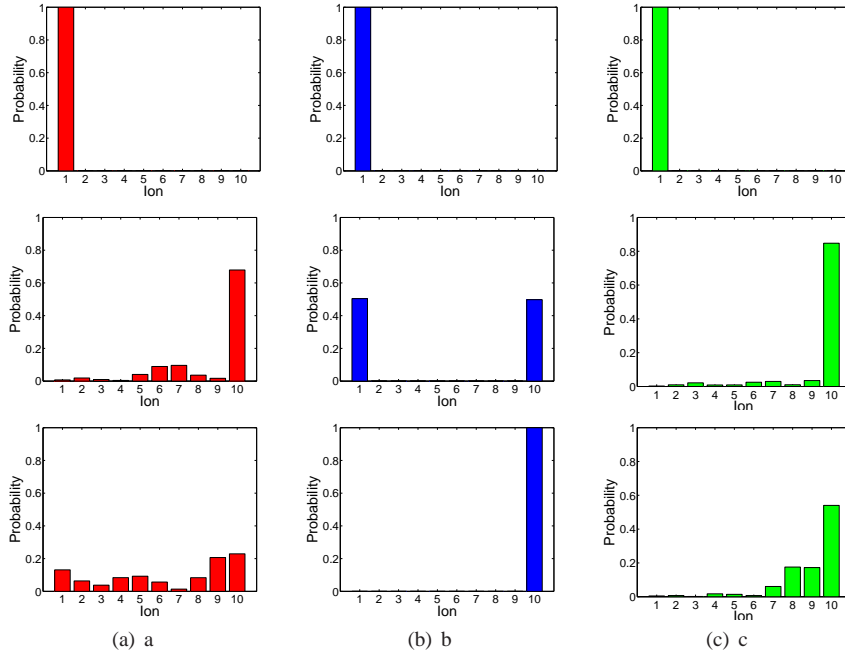


Figure 5. Leftmost histograms: probability amplitude of a single excitation (phonon) across the chain, if the evolution occur for frequencies $\omega_j = 50\omega_L \forall j$ after times (from top to bottom) $t = 0$, $t = 375\omega_L^{-1}$ and $t = 5600\omega_L^{-1}$. Middle histograms: probability amplitude of a single excitation (phonon) across the chain, if the evolution occur for frequencies $\omega_1 = \omega_{10} = 5\omega_L$ and $\omega_j = 50\omega_L^{-1}$ for $j \neq 1, 10$ after times (from top to bottom) $t = 0$, $t = 2800\omega_L^{-1}$ and $t = 5600\omega_L^{-1}$. Rightmost histograms (red): probability amplitude of a single excitation (phonon) across the chain, if the evolution occur for frequencies $\omega_j = 10\omega_L \forall j$ after times (from top to bottom) $t = 0$, $t = 625\omega_L^{-1}$ and $t = 640\omega_L^{-1}$.

the sender has its qubit state encoded in the single excitation sector of the oscillations of the first ion (*i.e.*, on the subspace spanned by the phonon states $|0\rangle$ and $|1\rangle$) and wants to send the excitation through the chain to a receiver who owns the last ion. Notice that, as recalled in Sec. 3.2, a (non-Gaussian) single qubit state of this kind could be prepared, in practice, by coupling the motion of an ion to the internal degrees of freedom through a proper sequence of blue and red sideband pulses.

Neglecting, for the time being, thermal noise (see below), one has that the state $|0\rangle$ can be sent perfectly through the chain. Therefore, the overall fidelity of the transmission depends solely on the fidelity with which $|1\rangle$ can be sent from the first to the last ion. The amplitude of such a transfer can be determined analytically by tracking the evolution of the initial operator a_1^\dagger (creating the excitation in the first ion) in Heisenberg picture. Because the system is harmonic the evolution of a_1^\dagger results in a linear combination of field operators, which can be determined with standard techniques. We could thus consider different situations. The histograms we plot show the probability amplitude P for finding a single excitation at different sites in the chain. The resulting transmission fidelity (averaged over the Haar measure of a single qubit space) is given by $1 - \frac{1}{2}(1 - \sqrt{P})^2 + \frac{3}{4}\sqrt{P}(1 - \sqrt{P})$, monotonically increasing with P . We will consider a chain of $n = 10$ ions and an initial ground state for trapping frequencies $\omega_j = 50\omega_L \forall j$.

Fig. 5(a). shows the case where the trapping frequencies are left unchanged after the initial preparation. Because the interacting terms, while very small, are still present, the excitation propagates because the local mode of the first ion is not exactly a normal mode of the system. After an evolution time $t = 375\omega_L^{-1}$, 0.76 of the probability amplitude is transferred to the final state. However, the propagation is rather dispersive, as each mode is on resonance with all the others.

In order to boost the probability of transmitting the excitation, sender and receiver can switch the local trapping frequencies of their respective ions from the initial value $\omega_i = 50\omega_L$ down to a common value ω_f : in this way they can realise the beam splitting operation at distance described in Sec. 3.1.3 which, in principle, would allow for perfect swapping. This specific example thus also illustrates our previous general discussion and shows with which precision and over which operating times are linear operations actually possible over a chain of ions. As one can see from Fig. 5(b), where $\omega_f = 5\omega_L$ has been assumed, the beam splitting operation is virtually perfect: all the probability amplitude is gradually transferred to the final ion, while the other ions are never involved in the process. This quality in the transfer comes at the expense of transfer time: over 10 ions the beam splitting operation takes roughly an order of magnitude more ($t \simeq 5600\omega_L^{-1}$) than the imperfect transfer considered in Fig. 5(a). This is simply due to the fact that, by keeping the middle ions on resonance, one takes advantage of the interaction between nearby ions, which are clearly stronger (as the interaction decays like the cube of the distance) and propagate the excitation through the chain. For given trapping frequencies, the time needed to achieve the beam splitter between radial modes at the two end of a chain of n ions scales very accurately as n^2 . Notice also, as a side remark, that since the Coulomb corrections to the local trapping frequencies are symmetric with respect to the longitudinal centre of the trap, the transfer between extremal ions is somewhat favoured in practice, as equal trapping potentials will result in equal effective trapping frequencies for such ions.

Finally, in Fig. 5(c), we consider a ‘compromise’ between the two cases analysed above: all the frequencies are changed to the frequency $10\omega_L$ obtaining, after a time $t = 625\omega_L^{-1}$, a transferred probability amplitude of 0.85. It is important to remark that the slower beam splitting operation, where the quantum information does not disperse through the chain at all, is not only more precise than the other two options examined, but also much more stable with respect to imperfections in the allowed interaction times.

Let us now turn to inspect the effect of decoherence: clearly, thermal phonons are deleterious for the transfer of information encoded in single excitation sectors. The analytical estimates for the transfer times we just presented allow us to determine the restrictions on the heating rates that would allow such systems to transfer information in practical situations. Assuming a longitudinal trapping frequency of 1 MHz and a (less ambitious) chain of 5 ions, one would realise a beam splitting operation (perfect transfer) between extremal ions in $t \simeq 1.4\text{msec}$. In such a case, heating rates as low as $\epsilon \simeq 0.1$ kHz would be needed for a coherent transfer to take place. For such heating rates, the action of the thermal phonons on the fidelity between initial and final state can be assumed to be linear resulting, after average over the Haar measure, into a mean fidelity $\mathcal{F} \simeq 1 - 3\epsilon t/2 \simeq 0.8$. Such heating rates are certainly demanding for arrays of traps, but not inconceivable, considering the heating rates achieved for single traps and the fact that current systems all operate at room temperature

The effect of losses and thermal phonons for small ϵ (so that $\epsilon t \ll 1$ over the interesting time-scales) can be easily estimated by letting the master equation Eq. (4) for $N \gg 1$ act at first order on an otherwise perfectly transferred generic state $\alpha|0\rangle + \beta|1\rangle$, and by setting $\epsilon = \gamma N$. The fidelity between initial and final states (corresponding to the overlap, for pure initial state) can be then determined and averaged over the Haar measure of a single qubit Hilbert space, to obtain the mean value $\mathcal{F} \simeq 1 - 3\epsilon t/2$.

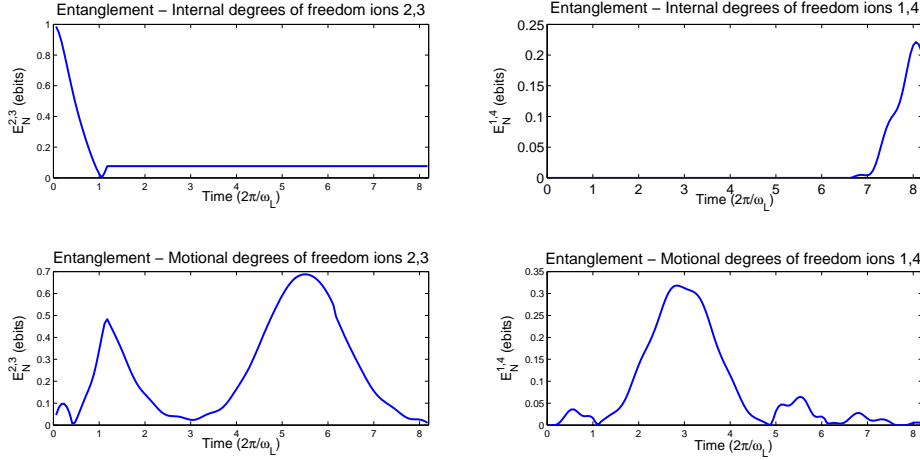


Figure 6. Propagation of the entanglement (logarithmic negativity) between internal and motional degrees of freedom. The initial state is a Bell singlet between the internal degrees of freedom of the second and the third ions; the transverse trapping frequency is $10\omega_L$. The upper (lower) plot on the left column shows the logarithmic negativity between the internal (motional) degrees of freedom of ions 2 and 3. The upper (lower) plot on the right column shows the logarithmic negativity between the internal (motional) degrees of freedom of ions 1 and 4. The dynamics is divided into three stages. In the first stage (for $0 \leq t \leq 1.2\frac{2\pi}{\omega_L}$), the coupling between internal and motional degrees of freedom of ions 2 and 3 is on, and the entanglement is swapped from the former to the latter. In the next stage (for $1.2\frac{2\pi}{\omega_L} \leq t \leq 6.2\frac{2\pi}{\omega_L}$), all the internal and motional degrees of freedom couplings are off, and the entanglement propagates through the chain via the motional degrees of freedom. Finally, for $t \geq 6.2\frac{2\pi}{\omega_L}$, the coupling between internal and motional degrees of freedom of ions 1 and 4 is on, and the final swapping takes place.

(thus, in principle, two orders of magnitude could be gained on heating rates).

5.2. The role of the internal degrees of freedom

In the preceding section, while discussing the transfer of finite dimensional quantum information, we started off from a situation where a qubit state is encoded in the first two number states of the first ion. As already mentioned above, one of the most expedient ways to create such a finite dimensional state for the motional degrees of freedom is creating the desired state for the ‘internal’ degrees of freedom of the ion (embodied by its internal electronic levels) and then coupling them to the local radial modes to achieve the swapping. In order to provide the reader with a more comprehensive treatment and give him/her a flavour of the way the internal degrees of freedom enter in such dynamics, we briefly give account of a specific example where the internal degrees of freedom are involved throughout the whole transmission of quantum information.

We shall consider a trap with four ions, with $\omega_j = 10\omega_L$ for $1 \leq j \leq 4$. To keep the example down to earth, we will not assume any capability of local control nor any change during the evolution for the radial frequencies here. The only manipulation required will be the switching on and off of the coupling between the local phonons and the two levels of each ion where the initial qubit state is encoded. Denoting such levels $|e\rangle_j$ and $|g\rangle_j$, and setting $\sigma_{x,j} := |e\rangle_j\langle g|_j + |g\rangle_j\langle e|_j$, we shall assume the following interaction Hamiltonian \hat{H}_j^{int} for

each ion j :

$$\hat{H}_j^{int} = g_j \sigma_{x,j} \hat{X}_j,$$

which describes appropriately the coupling realised in experiments (see, *e.g.*, [19]). For simplicity, the interaction strengths g_j will be all set to ω_L (notice that, because the oscillators' frequency are set to $10\omega_L$, the interaction reduces, up to a very good approximation, to a rotating wave one). As initial state, at $t = 0$, we assume a Bell state between the internal degrees of freedom of ions 2 and 3, and the ground state for the remainder of the system:

$$|g\rangle_1 \otimes (|g\rangle_2 \otimes |e\rangle_3 + |e\rangle_2 \otimes |g\rangle_3) \otimes |g\rangle_4 \otimes \varrho_g,$$

where ϱ_g is the ground state of the radial modes of the ions. As a signature for the transmission of quantum information, we will consider the evolution of the entanglement between the internal and motional degrees of freedom of ions 2 – 3 (initially entangled) and ions 1 – 4 (which gets entangled through the process), which is reported in Fig. 6 in terms of logarithmic negativity (the logarithmic negativity between internal degrees of freedom of ions j and k is denoted $\tilde{E}_N^{j,k}$). The dynamics is then split into three stages: from time $t = 0$ to $t = 1.2 \cdot 2\pi/\omega_L$ the internal and motional degrees of freedom of ions 2 and 3 are coupled and the entanglement is dynamically swapped from the former to the latter. Next, from $t = 1.2 \cdot 2\pi/\omega_L$ to $t = 6.2 \cdot 2\pi/\omega_L$, the coupling is switched off and the entanglement propagates through the chain via the motional degrees of freedom, and the radial modes of ions 1 and 4 get entangled. Finally, from $t = 6.2 \cdot 2\pi/\omega_L$ to $t = 10 \cdot 2\pi/\omega_L$, the entanglement is swapped to the internal degrees of freedom of ions 1 and 4. One can see that, though the quantum information partially disperses under such conditions (essentially due to the stringent restrictions we put, in this instance, on the control of the local frequencies), the process is capable of transferring the entanglement from the internal degrees of freedom of ions 2 and 3 to those of ions 1 and 4 through the radial motional degrees of freedom.

5.3. Propagation of continuous variable states and entanglement

Clearly, quantum information (and entanglement) can be propagated through the chains under examination also at a continuous variable level, when populating the whole infinite dimensional Hilbert space. The study of information and entanglement propagation over harmonic chains has been proposed and discussed in detail in [37, 39]. Here, we shall investigate cases of such propagations along the chains of ions we are considering, addressing specific instances which can be realised in the laboratory. Our aim is pointing out at what degree and under what conditions can the theoretical schemes based on harmonic chains be implemented on radial modes of trapped ions.

As argued in [37], the capacity of transmitting quantum states between distant parties is closely related to the capacity of transmitting, or “swapping”, entanglement between them. In fact, the latter also critically requires the transfer to happen coherently through the whole process. In view of this fact we will limit ourselves to consider the propagation of CV entanglement (rather than the fidelity between sent and received quantum states). Also, in order to focus on a feasible scenario, we shall consider a common initial condition: the chain of n ions starts off from the (completely separable) ground state for $\omega_j = \omega_0 \forall j$ and, then, entanglement between the first and the second ion is created, as described in Sec. 4, by switching their frequencies to the same frequency ω_e . From now on the first ion is left off-resonance at frequency ω_e (and thus effectively isolated from the chain), and the aim is transmitting its initial entanglement with the second ion through the chain over to the final n -th ion. Two options will be examined:

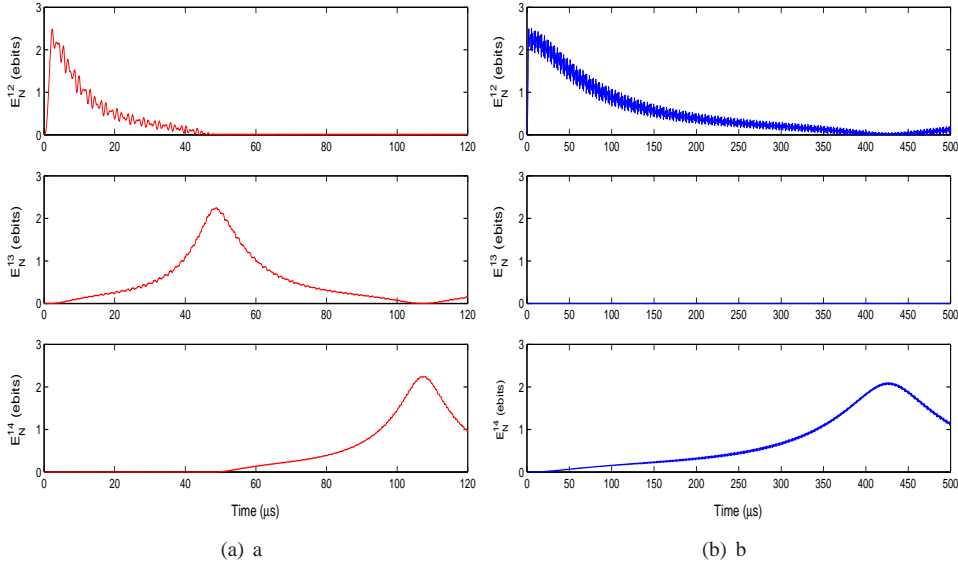


Figure 7. Transfer of the entanglement with the first ion of a chain (measured by ebits of logarithmic negativity E_N^{jk}) from the second ion to the last one, in a chain of four ions. From top to bottom, the plots show the entanglement between ions 1 and 2 (E_N^{12}), 1 and 3 (E_N^{13}) and 1 and 4 (E_N^{14}). On the left side (a), the entanglement is transferred by a relay of beam splitters obtained by switching the radial trapping frequencies of the ions 2 and 3 to $\sqrt{98.8}\omega_L$ for a time $46\omega_L^{-1}$ while keeping the other ions off-resonant and then, finally, by switching the trapping frequencies of ions 3 and 4 to $\sqrt{98.8}\omega_L$ (with the other ions off-resonant). On the right side (b), the entanglement is transferred directly by a beam-splitter between ions 2 and 4, obtained by setting their frequencies to $\sqrt{98.8}\omega_L$ while keeping the others off resonance. In both cases, the state at time $t = 0$ is the ground state for all trapping frequencies equal to $\sqrt{98.8}\omega_L$ (such a value takes into account the corrections due to Coulomb repulsions) and, during the initial $2 \mu\text{s}$, the entanglement between ions 1 and 2 is built up by bringing their ‘bare’ trapping frequencies down to $2 \mu\text{s}$.

- i) the entanglement is swapped by a chain of beam splitters between neighbouring ions (achieved by setting such neighbouring ions at the original frequency while putting the others off-resonance);
- ii) the entanglement is swapped directly by a beam splitter between the ions at the far ends of the chain.

Notice that in case i) the beam-splitters operate at the original frequency ω_0 so that no local squeezing takes place, as evident from Eq. (5). Local squeezing would affect the entanglement between the modes but also, crucially, alter the original state to be transmitted and is thus undesirable in the present context.

The two strategies i) and ii) are compared in Fig. (7) for a chain of four ions. Such a small system already permits one to highlight all the essential features of the two strategies. As apparent, a complete dynamical swapping of the entanglement can be achieved in both cases, with remarkable accuracy. A chain of beam splitters allows for a faster transfer, as one should expect since the coupling κ_{jk} between distant ions is inversely proportional to their cubed distance: in general, the time needed to send information across n ions by a ‘relay’ of beam splitters roughly scales like n , whereas the time needed to achieve a beam-splitting operation between first and last ion scales like n^3 . A ‘relay’, taking less time, is thus less sensitive to

decoherence and dissipation. On the other hand, a single beam-splitting operation between distant ions only requires a single adjustment of the trapping frequencies (after the initial entanglement is created), whereas a chain of beam-splitters requires $n - 2$ manipulations, which would be possibly difficult to master in practice and could involve more errors and imperfections. Therefore, we have investigated the effect of imperfections in frequencies and evolution times on the transfer for both cases: the series of beam-splitters turns out to be more robust. In the instance depicted in Fig. 7, the transfer by a series of beam-splitters is left virtually unaffected by uncertainties of $0.1\omega_L$ on frequencies and $0.1\omega_L^{-1}$ on operating times (ω_L is the longitudinal trapping frequency) whereas, on average, the entanglement transferred by a single beam splitter is reduced to $\simeq 1.2$ ebits of logarithmic negativity (out of $\simeq 2.2$ ebits initially present between ions 1 and 2) by the same imperfections. Summing up, strategy i) proved to be more reliable and faster (and thus less subject to decoherence and dissipation) and is hence to be preferred for the transmission of CV quantum information over chains of ions. Considering once again the example of Fig. 7, for a longitudinal frequency $\omega_L = 1$ MHz, an effective coherent transfer would take about $100 \mu\text{s}$ and thus require heating rates around 1 KHz to be carried out effectively.

6. Nonlocality tests

The presence of strong Gaussian multipartite entanglement highlighted in Sec. 4 can be experimentally demonstrated and put to use in testing quantum nonlocality. Central to this endeavour is the capability of performing non-Gaussian measurements on the motional state of the ions, pointed out in Sec. 3.2. In particular, we already recalled that phonon-number parity measures are possible on single copies of the system, and so are displacement operations. In this section, we will explore the possibility of violating multipartite Bell-like inequalities (the so-called ‘‘Klyshko’’ inequalities [43]) by measuring ‘‘displaced parity’’ observables, as proposed for generic CV systems by Banaszek and Wodkiewicz [44]. Although bound to be subject to the locality loophole (considering that the distances between the ions are typically of the order of $1 \mu\text{m}$), such an experiment would be a remarkable test of quantum non-locality with massive particles, which is still lacking.

To fix ideas and address a situation within the reach of current experiments, we shall study the test on the three-mode Gaussian state whose entanglement is described in Fig. 3, setting the evolution time to $t = 5 \mu\text{s}$ and the heating rate to $\epsilon = 200 \text{Hz}$ (resulting from a coupling to the bath $\gamma = 10^{-4} \text{Hz}$ and a temperature $T = 294^\circ \text{K}$), whose CM will be denoted by σ_3 . The family of (non-Gaussian) local, bounded, dichotomic observables for the displaced parity test is given by $\Pi_j(x_j, p_j) \equiv \hat{D}_j(x_j, p_j)^\dagger (-1)^{\hat{n}_j} \hat{D}_j(x_j, p_j)$, where \hat{D}_j and \hat{n}_j are respectively the displacement and number of phonons operators of ion j . The three observers, pertaining to the three ions, randomly apply two different displacements [$\hat{D}_j(x_j, p_j)$ and $\hat{D}_j(x'_j, p'_j)$] on their ions and then measure parity locally. Such a measurement is clearly non-Gaussian, and allows one to violate Bell inequalities with Gaussian states. The expectation value of the operator $\Pi(R) \equiv \Pi_1(x_1, p_1) \otimes \Pi_2(x_2, p_2) \otimes \Pi_3(x_3, p_3)$ is simply proportional to the Wigner function $W(R)$ of the composite system evaluated in the point $R = (x_1, x_2, x_3, p_1, p_2, p_3)^\text{T}$: $\langle \Pi(R) \rangle = (2/\pi)^3 W(R)$ [45]. For a three-mode Gaussian state with covariance matrix σ_3 one has

$$W(R) = e^{-\frac{1}{2}R^\text{T}\sigma_3^{-1}R} / (\pi^3 \sqrt{\text{Det } \sigma_3}).$$

The Bell-Klyshko inequality finally reads:

$$B_3 \equiv \frac{8}{\pi^3} |W(x_1, x_2, x'_3, p_1, p_2, p'_3) + W(x_1, x'_2, x_3, p_1, p'_2, p_3)|$$

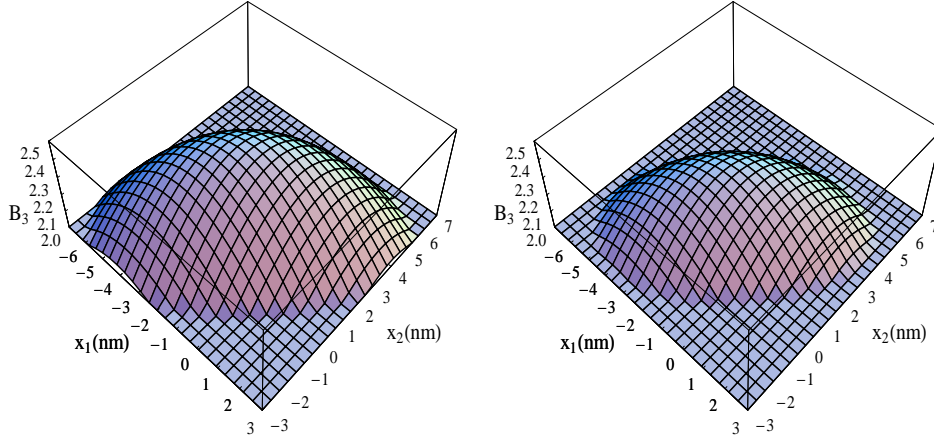


Figure 8. Function B_3 for $p_1 = p_2 = p_3 = p'_1 = p'_2 = p'_3 = 0$, $x'_1 = x'_3 = 6\text{nm}$, $x'_2 = -4\text{nm}$, $-7\text{nm} \leq x_1 = x_3 \leq 3\text{nm}$ and $-3\text{nm} \leq x_2 \leq 7\text{nm}$ for the three-mode Gaussian state obtained as detailed in the caption of Fig. 3 after a time $t = 5\mu\text{s}$. On the left hand-side no dissipation is accounted for, while on the right-hand side a heating rate $\epsilon \simeq 200\text{Hz}$ is introduced. Dimensions were reintroduced assuming $\omega_L = 1\text{MHz}$ and Ca ions. The plane $B_3 = 2$, above which violation occurs, is the bottom of the plots; in the displayed region, the functions reach maxima of $\simeq 2.45$ for the pure state case and of $\simeq 2.28$ with dissipation.

$$+ W(x'_1, x_2, x_3, p'_1, p_2, p_3) - W(x'_1, x'_2, x'_3, p'_1, p'_2, p'_3)| \leq 2. \quad (6)$$

Quantum mechanics allows for $2 \leq B_3 \leq 4$.

Fig. 8 show a region in the space of displacements where the violation of the inequality is substantial and remarkably stable. It is apparent that, for such choices of displacements, the tolerable error on the displacement operation needed to maintain the violation is around 1.5nm , which is within reach of current experimental capabilities. Also, as shown in the plot on the right, heating rates of 200Hz are still compatible with a violation of the inequalities.

This preliminary study reveals very promising perspectives concerning the violation of Bell inequalities with massive degrees of freedom. Even if subject to a locality loophole, this endeavour would still stand out as a major, not yet probed, testing ground for fundamental quantum mechanics [46], and epitomises the considerable promise radial modes hold for quantum information and fundamental investigations alike.

7. Summary and outlook

We demonstrated how the local control of the trapping frequencies would allow one to reproduce any linear optical manipulation on radial modes of trapped ions. Drawing from previous studies on similar settings, we pointed out that phonon detection and homodyne detection as well as the implementation of non-Gaussian operations is possible in this setting. Next, we emphasized that, even restricting to global control, such manipulations enjoy a high efficiency in entanglement generation and a considerable resilience in the face of currently achievable dissipation rates. We then made manifest that radial modes could be used for the transmission of quantum information, stored in finite dimensional subspaces of the bosonic Hilbert space as well as in the full continuous variable domain. Finally we showed that, through (achievable) measurements of the displaced parity operator, Bell-like inequalities can

be violated under realistic decoherence and dissipation rates. As a rule of thumb, applying to systems with $n \simeq 6$ ions or less and longitudinal trapping frequencies $\omega_L \simeq 1$ MHz, our study indicates that heating rates around 1 KHz are sufficiently low for coherent manipulations and robust entanglement generation in the continuous variable regime, whereas non-locality tests and transmission of finite-dimensional quantum dimensional information (stored in single phonons) are more delicate, requiring heating rates around 100 Hz to be carried out efficiently.

In the light of the above, the experimental pursuit of the presented programme holds considerable promise, concerning both technological developments, such as the storage and manipulation of quantum information or the efficient generation of entanglement, and tests of fundamental physical aspects, as in the nonlocality test for massive degrees of freedom here discussed. As a first step to push this analysis further, a study is currently under way to examine the possibility to swap the remarkable entanglement produced in the traps to light modes, to ultimately beat parametric processes in the generation of quantum optical CV entanglement [17].

Acknowledgments

We thank F.G.S.L. Brandão, T. Coudreau, H. Häffner, M. Keller, W. Lange, K. Pregnell, D.M. Segal and R.C. Thompson for helpful discussions. This work has been supported by the European Commission under the Integrated Project QAP, funded by the IST directorate as Contract Number 015848, by an EU Marie Curie IEF fellowship, by the EU STREP project CORNER, by the Royal Society and is part of the EPSRC QIP-IRC and by EPSRC project number EP/E045049/1.

- [1] S. L. Zhu, C. Monroe, and L. M. Duan, *Phys. Rev. Lett.* **97**, 050505 (2006).
- [2] C. F. Roos, T. Monz, K. Kim, M. Riebe, H. Häffner, D. F. V. James, and R. Blatt, *Phys. Rev. A* **77**, 040302(R) (2008).
- [3] D. F. V. James, *Appl. Phys. B* **66**, 181 (1998).
- [4] J. Eisert and M. B. Plenio, *Int. J. Quant. Inf.* **1**, 479 (2003).
- [5] M. B. Plenio and S. Virmani, *Quantum Inf. Comp.* **7**, 1 (2007).
- [6] See, *e.g.*, A. Serafini, M. G. A. Paris, F. Illuminati, and S. De Siena, *J. Opt. B* **7**, R19 (2005).
- [7] S. Stahl, F. Galve, J. Alonso, S. Djekic, W. Quint, T. Valenzuela, J. Verdu, M. Vogel, and G. Werth, *Eur. Phys. J. D* **32** 139 (2005).
- [8] G. Ciaramicoli, F. Galve, I. Marzoli, and P. Tombesi, *Phys. Rev. A* **72**042323(2005).
- [9] S. Schulz, U. Poschinger, K. Singer, F. Schmidt-Kaler, *Fortschr. Phys.* **54**, 648 (2006); G. Huber, T. Deuschle, W. Schnitzler, R. Reichle, K. Singer, F. Schmidt-Kaler, *New J. Phys.* **10**, 013004 (2008).
- [10] See J. Labaziewicz, Y. Ge, P. Antohi, D. Leibbrandt, K. R. Brown, and I. L. Chuang, *Phys. Rev. Lett.* **100**, 013001 (2008).
- [11] D. J. Heinzen and D. J. Wineland, *Phys. Rev. A* **42**, 2977 (1990).
- [12] J. I. Cirac, A. S. Parkins, R. Blatt, and P. Zoller, *Phys. Rev. Lett.* **70**, 556 (1993).
- [13] E. Solano, *Phys. Rev. A* **71**, 013813 (2005).
- [14] Arvind, B. Dutta, N. Mukunda, and R. Simon, *Pramana J. Phys* **45**, 471 (1995).
- [15] M. Reck, A. Zeilinger, H. J. Bernstein and P. Bertani, *Phys. Rev. Lett.* **73**, 58 (1994).
- [16] Y. Takeno, M. Yukawa, H. Yonezawa, and A. Furusawa, *Optics Express* **15**, 4321 (2007).
- [17] A. Serafini, A. Retzker, and M. B. Plenio, in preparation.
- [18] S. L. Braunstein and P. van Loock, *Rev. Mod. Phys.* **77**, 513 (2005).
- [19] D. M. Meekhof, C. Monroe, B. E. King, W. M. Itano, and D. J. Wineland, *Phys. Rev. Lett.* **76**,1796 (1996).
- [20] S. Wallentowitz and W. Vogel, *Phys. Rev. Lett.* **75**, 2932 (1995).
- [21] J. F. Poyatos, R. Walsler, J. I. Cirac, P. Zoller, and R. Blatt, *Phys. Rev. A* **53**(4), R1966 (1996).
- [22] P. J. Bardroff, C. Leichtle, G. Schrade, and W. P. Schleich, *Phys. Rev. Lett.* **77**, 2198 (1996).
- [23] S. Gleyzes, S. Kuhr, C. Guerlin, J. Bernu, S. Deléglise, U. B. Hoff, M. Brune, J.-M. Raimond, and S. Haroche, *Nature* **446**, 297 (2007).
- [24] D. Achilles, Ch. Silberhorn, and I. A. Walmsley, *Phys. Rev. Lett.* **97**, 043602 (2006); D. Achilles, Ch. Silberhorn, C. Sliwa, K. Banaszek, I. A. Walmsley, M. J. Fitch, B. C. Jacobs, T. B. Pittman, and J. D. Franson, *J. Mod. Opt.* **51**, 1499 (2004); J. S. Lundeen, A. Feito, H. Coldenstrod-Ronge, K. L. Pregnell, Ch. Silberhorn, T. C. Ralph, J. Eisert, M. B. Plenio, I. A. Walmsley, arXiv:0807.2444 (2008).

- [25] E. Waks, E. Diamanti, B. C. Sanders, S. D. Bartlett, and Y. Yamamoto, *Phys. Rev. Lett.* **92**, 113602 (2004); E. Waks, E. Diamanti, and Y. Yamamoto, *New J. Phys.* **8**, 4 (2006).
- [26] D. J. Wineland, R. E. Drullinger, and F. L. Walls, *Phys. Rev. Lett.* **40**, 1639 (1978).
- [27] C. Monroe, D. M. Meekhof, B. E. King, S. R. Jefferts, W. M. Itano, D. J. Wineland, and P. Gould, *Phys. Rev. Lett.* **75**, 4011 (1995).
- [28] G. Morigi, J. Eschner and C.H. Keitel, *Phys. Rev. Lett.* **85**, 4458 (2000).
- [29] A. Retzker and M. B. Plenio, *New J. Phys.* **9**, 279 (2007).
- [30] J. Eisert, M. B. Plenio, S. Bose, J. Hartley, *Phys. Rev. Lett.* **93**, 190402 (2004).
- [31] J. Eisert and M.B. Plenio, *J. Mod. Opt.* **46**, 145 (1999); J. Lee, M. S. Kim, Y. J. Park, and S. Lee, *J. Mod. Opt.* **47**, 2151 (2000); G. Vidal and R. F. Werner, *Phys. Rev. A* **65**, 032314 (2002); J. Eisert, PhD Thesis (Universität Potsdam, 2001); M. B. Plenio, *Phys. Rev. Lett.* **95**, 090503 (2005).
- [32] G. Giedke, B. Kraus, M. Lewenstein, and J. I. Cirac, *Phys. Rev. A* **64**, 052303 (2001).
- [33] A. Garg, *Phys. Rev. Lett.* **77**, 964 (1996).
- [34] L. Deslauriers, S. Olmschenk, D. Stick, W. K. Wootters, J. Sterk, and C. Monroe, *Phys. Rev. Lett.* **97**, 103007 (2006).
- [35] J. Laurat, G. Keller, J. A. Oliveira-Huguenin, C. Fabre, T. Coudreau, A. Serafini, G. Adesso, and F. Illuminati, *J. Opt. B* **7**, S577 (2005).
- [36] V. Coffman, J. Kundu, and W. K. Wootters, *Phys. Rev. A* **61** 052306 (2000); B. M. Terhal, *IBM J. Res. & Dev.* **48** 71 (2004); G. Adesso and F. Illuminati, arXiv:0805.2942 (2008).
- [37] M.B. Plenio, J. Hartley, J. Eisert, *New J. Phys.* **6**, 36 (2004)
- [38] X. M. H. Huang, C. A. Zorman, M. Mahregany, and M. L. Roukes, *Nature* **421**, 974 (2003).
- [39] M. B. Plenio and F. L. Semião, *New J. Phys.* **7**, 73 (2005).
- [40] D. Porras and J. I. Cirac, *Phys. Rev. Lett.* **93**, 263602 (2004); *ibid.* **92**, 207901 (2004).
- [41] A. Retzker, R. Thompson, D. Segal, and M.B. Plenio, arXiv:0801.0623 (2008).
- [42] S. Bose, *Contemp. Phys.* **48**, 13 (2007); D. Burgarth, PhD Thesis (University College London, 2006), arXiv:0704.1309.
- [43] N. D. Mermin, *Phys. Rev. Lett.* **65**, 1838 (1990); D. N. Klyshko, *Phys. Lett. A* **172**, 399 (1993).
- [44] K. Banaszek and K. Wodkiewicz, *Phys. Rev. A* **58**, 4345 (1998).
- [45] S. M. Barnett and P. M. Radmore, *Methods in Theoretical Quantum Optics* (Oxford University Press, Oxford, 1997), pag. 118.
- [46] A. Retzker, I. J. Cirac and B. Reznik, *Phys. Rev. Lett.* **94**, 050504 (2005).